

Glauber Calculations of Centrality Dependent Variables in Au+Au collisions at $\sqrt{s_{NN}} = 200$ GeV (Run 7)

Rui Wei¹, Roy Lacey¹, Arkadij Taranenko¹, Jiangyong Jia¹
Maya Shimomura², ShinIchi Esumi²
Alexander Milov³

¹Stony Brook University

²University of Tsukuba

³Weizmann Institute

February 13, 2009

Abstract

This note describes the procedure employed to generate Glauber-based model extractions of average values for the impact parameter ($\langle b \rangle$), number of participants ($\langle N_{\text{part}} \rangle$), number of collisions ($\langle N_{\text{coll}} \rangle$), standard eccentricity ($\langle \varepsilon_{\text{std}} \rangle$) and participant eccentricity ($\langle \varepsilon_{\text{part}} \rangle$) and transverse size \bar{R} for centrality selections made with the BBC charge percentile method in Run 7 (Au+Au collisions at $\sqrt{s_{NN}} = 200$ GeV). Tabulated results are presented in conjunction with systematic error estimates. These results are compared to previous official Glauber quantities. We also compare the PHENIX Glauber code to the PHOBOS Glauber code in detail.

Contents

1	Introduction	2
2	Comments on PHENIX Minimum Bias efficiency	2
3	The Glauber Monte-Carlo approach	3
3.1	Relating the Glauber model quantities to experimental data	3
3.2	Glauber Monte Carlo approach for Run 7 BBC charge-percentile centrality classes	4
3.3	Calculating Glauber Parameters	5
3.4	Evaluation of systematic errors	11
4	Appendix A: Comparison between PHENIX and PHOBOS Glauber MC	17
5	Appendix B: Data driven NBD and its dependence on bbc z vertex	21
6	Appendix C: Participant eccentricity a la PHOBOS	24
6.1	Standard Eccentricity	24
6.2	Participant Eccentricity	24

1 Introduction

In PHENIX, BBC and ZDC are used to provide the minimum bias trigger and centrality determination. Over the course of past eight years, several centrality determination methods have been developed. 1) Perp method which defines centrality by applying cut perpendicular to the BBC charge vs ZDC energy. 2) Clock-method which defines centrality by cut on the angle ϕ of a given (BBC,ZDC) value relative to a fixed origin, typically chosen to be $(0.2BBC_{max}, 0)$. 3) BBC-percentile method which defines centrality by cutting only on the BBC charge. 4) BBC-based absolute centrality method, where the all events are sliced monotonically according to N_{part} value determined event by event from BBC charge. Efficiency is folded in such the centrality that is defined in 0-100% range.

Perp method was used in PPG001, Clock method has been the standard in all previous Au+Au runs at 200 GeV. BBC-percentile method was used in Au+Au 62.4 GeV, Cu+Cu at 200 and 62.4 GeV, as well as d+Au collisions. People have since realized that the BBC percentile method have certain advantages over the Clock method. For example, it was demonstrated by Sasha in Analysis note 461 that the requirement of ZDC in the centrality definition introduces large RMS width on the N_{part} and N_{coll} in the peripheral bin. Hence it was decided in a recent analysis meeting that BBC percentile method should be used for RUN 7 analysis. Method 4) could be used for a latter run, once all the systematics associated with the method are understood.

There are several reasons why the Glauber quantities need to be re-determined for RUN 7. 1) Previous official Glauber quantities for Au+Au at 200 GeV was done using Clock method, they need to be re-calculated for BBC percentile method. 2) Previous Glauber quantities only include N_{part} , N_{coll} , b , T_{AB} and ϵ_{std} . In this note, we also calculated several additional useful variables. Their values and associated systematic errors need to be evaluated. 3) We are using a hybrid Glauber model which is based on published PHOBOS Glauber model, but include detector response from PHENIX Glauber. A number of improvements have been included.

2 Comments on PHENIX Minimum Bias efficiency

The minimum bias trigger condition for all 200 GeV Au+Au was defined as: $bbc_n \geq 2 \& \& bbs \geq 2 \& (ZDCNS|ZDCLL1)$ (ZDC hit required Level-1 live bit in TriggerHelper).

In Analysis note 103 [1], Kensuke Homma have used HIJING simulation at 200 GeV Au+Au to estimate the trigger efficiency, where the simulated HIJING events were run through a GEANT simulation of the BBC response. The vertex distribution for these events was chosen to approximate what was seen during real data taking. From these events, Kensuke Homma has estimated a efficiency of $92.3 \pm 0.4(stat) \pm 1.6(sys)$. As far as we know, the BBC response haven't changed over the years, so this study should largely remain valid.

There were concerns about possible contamination from background events that were generated by a BBC after-pulse, such that the readout electronics of other detectors to report non-zero data. These data could distort the physics results significantly. They were mostly removed by selecting on the correct bunch crossing [2, 3]. This was done by BunchCross class in the reconstruction stage. The remaining fraction of BBC accepted events which were rejected by ZDC is on the order of 1-2% [2]. However it was not clearly how much of those was genuine real events, currently it was simply considered as additional systematic uncertainties on the trigger efficiency.

In RUN2 the trigger efficiency was set at 92.4%. In RUN4, the minimum bias efficiency was chosen to be 93%¹. Sasha Milov have done an independent detailed fits using Negative Binomial Method [4], in which obtained a fit efficiency 92%. But if he then calculated the efficiency using a Glauber simulation where N_{part} is folded with NBD using the fit parameter, and superimposed with the trigger requirement, he got a efficiency of 94.2%. In Run7, he repeat improved this study by taking into account the z vertex dependence [5]. The efficiency is determined to be 94%(from fit) to 96% (calculated from Glauber MC+NBD). The change from RUN4, however, is not necessarily means that the trigger efficiency is higher, it could simply means that the BBC gain calibration varies from RUN period to RUN period.

Until further detailed study is performed, we assume the minimum bias efficiency is $93\% \pm 2\%$ to be consistent with previous runs.

3 The Glauber Monte-Carlo approach

The Glauber Monte Carlo approach relevant to analyses' at RHIC has been recently reviewed [6]. Briefly, the A nucleons of nucleus A and B nucleons of nucleus B are assembled in a three-dimensional coordinate system (according to their respective nuclear density distribution) and following a random impact parameter (b) selection from the distribution $d\sigma/db = 2\pi b$, a simulated collision between both nuclei is initiated. This nucleus-nucleus collision is treated as a sequence of independent binary nucleon-nucleon collisions, i.e., the nucleons travel on straight-line trajectories and the inelastic nucleon-nucleon cross-section is assumed to be independent of the number of collisions a nucleon underwent before. Via this procedure, one is able to simulate experimentally observable quantities such as the BBC hit multiplicity, and hence, apply centrality cuts similar to those applied in the analysis of real data.

3.1 Relating the Glauber model quantities to experimental data

Experimental results are normally represented as a function of “geometric” quantities such as N_{part} , N_{coll} , etc. Therefore, it is desirable to extract mean values for these quantities for the respective classes of measured events. This is carried out via a mapping procedure involving the definition of centrality classes in both the measured and the calculated distributions; a subsequent step is then used to connect the mean values from the same centrality class in the two distributions. **The specifics of the methodology of this mapping procedure for the BBC charge-percentile centrality classes is our primary objective in this note.**

The assumption underlying the BBC charge centrality classes is that the impact parameter b is a monotonic function of the average BBC charge multiplicity. That is, for large b events (peripheral) we expect low charge multiplicity, whereas for small b events (central) we expect large charge multiplicity. Once the total integral of this charge distribution is known, centrality classes are defined by binning the distribution based upon the fraction of the total integral. The same procedure can then be applied to the Glauber-based distribution obtained via a large number of Monte Carlo trials. For each centrality class, the mean value of the Glauber geometric quantities (e.g., $\langle N_{part} \rangle$, $\langle \varepsilon_{part} \rangle$) for the Monte Carlo events can then be calculated. As is well known, this relatively straightforward procedure is only complicated by the actual details of event selection, an uncertainty in the total measured cross section, fluctuations in both the measured and calculated distributions, as well as a finite kinematic acceptance.

¹The change from 92.4 to 93 was not entirely clear to us

3.2 Glauber Monte Carlo approach for Run 7 BBC charge-percentile centrality classes

To map Monte Carlo simulation onto the data, we exploit the idea that the integrated charge measured by either of the BBCs is linearly proportional to the number of participants [5]. As emphasized in Ref. [5], linearity here means that each participant contributes equally. The number of hits in the detector is typically assumed to follow the statistics of the negative binomial distribution (NBD) and the parameters μ and k of this distribution can be extracted as a function of the location of the vertex (relative to the nominal crossing point) by fitting the experimental BBC hits distribution [for each vertex interval] with a Negative Binomial Distribution (NBD) convoluted with the probability to have a given number of participants obtained with the Glauber Monte Carlo. Extensive documentation of such fits can be found in Ref. [5, 4]. Here, μ gives a measure of the average number of hits per participant pair while k gives a measure of the magnitude of the fluctuations. With these parameters and the assumption that the charge signal deposited in the BBC, for each hit, follows a Landau type distribution [7], one can map the Glauber Monte Carlo hits distributions on to the experimental ones. Fig.4 in Ref. [5], shows an example of the quality of agreement achieved between the distributions for data and Monte Carlo respectively.

In PHENIX, the NBD are used for two distinct purposes:

- Together with other approaches, it provides an estimation of minimum bias trigger efficiency. The efficiency determined from An461 is 94.2%, while that from An645 is 96%. They are somewhat higher than the official number of 93%, but they agree within the assigned systematic errors.
- NBD can then be used to estimate the Glauber quantities such as N_{part} and N_{coll} . In this exercise, we generate a set of Monte-Carlo Glauber events, which is then required to pass the triggering condition. The μ and k (or combined with some other procedures) should be chosen such that the fraction of events passing this cut matches the minimum bias trigger efficiency of 93%.

Extensive studies of the NBD distributions have already been made in AN461 for RUN4 and AN461 for RUN7 [5, 4]. An645 has found the μ and k values have rather strong dependence on BBC z vertex. To estimate the influences of the vertex dependence on the estimation of Glauber quantities, we have compared the N_{part} and N_{coll} calculated with the vertex dependent NBD parameter and those calculated with a NBD whose μ and k are fixed at vertex position weighted average values. The differences are in fact very small as detailed in Appendix B. This suggests that we can ignore the vertex dependence in the evaluation of the Glauber variables².

Initially we thought we should directly use the experimentally determined μ and k , folded with the Glauber model to calculate all Glauber quantities. We later realize that the μ , k values determined from the data is rather sensitive to the BBC calibration, which could change from RUN to RUN. The fact that μ and k change from ($\mu = 4.00, k = 1.4$) in RUN4 (AN461) to ($\mu = 5.00, k = 1.65$) in RUN7 (AN645) attest to this fact. So in order to use them out of box, the detector response in glauber simulation (the GetPhenixBBCInfo function) should be tuned to match the real data. This is not done. In such case, we have two choices, we could either 1) chose a set of μ and k that reproduce the 93% in Glauber simulation, or 2) we use the μ

²It may still be very important in the estimation of the overall trigger efficiency

and k procedure from data, but then rejects additional peripheral events according to the BBC charge. Choice 2) is the one that was used by Klaus for official Glauber code ³.

Based on this consideration and to be consistent with what has been done in previous Glauber calculation, we have use the second approach, where **the default value of μ and k used in the Glauber simulation is chosen to be $\mu = 4.0$ and $k = 1.4$ from An461 which gives minimum bias efficiency of about 94.2%, we then keep 93% of the event by cutting on the simulated BBC charge signal.**

3.3 Calculating Glauber Parameters

Previous analysis use PHENIX code from Klaus Reygers [8, 9] to calculate Glauber quantities. In our study, we choose to calculate all quantities using the PHOBOS Glauber code which has been released to public [10]. We modified the package to include BBC response from Klaus, such that we can simulate the BBC trigger efficiency in the standard way. Important sanity checks have been performed to make sure the two set of Glauber code produce the identical results when the same input parameters were used. The difference was found to be less than 1% for all centrality bins. The details of this study are documented in Appendix A.

In the course of this check, we have found a couple of improvements in the PHOBOS glauber code in comparison with PHENIX glauber.

- In PHENIX glauber, the impact parameter is given before the position of all the nucleons are determined. However because of the intrinsic fluctuation, the real center determined by all thrown nucleons will be different from the initial position. Thus the initial central position lost its meaning. In PHOBOS glauber, the centers of Au nuclei are re-calculated by the center of mass of all nucleons. The two centers are readjusted such that their distance equal to the initial input impact parameter. This procedure eliminates the artificial fluctuation on b caused by the randomization step when distributing nucleons.
- There are three eccentricities that were calculated in the literature, standard eccentricity (ϵ_{std}), reaction plane eccentricity (ϵ_{rp}) and participant eccentricity (ϵ_{part}) [11].

$$\epsilon_{std} = \frac{\langle y^2 \rangle - \langle x^2 \rangle}{\langle y^2 \rangle + \langle x^2 \rangle} \quad (1)$$

$$\epsilon_{rp} = \frac{\sigma_y^2 - \sigma_x^2}{\sigma_y^2 + \sigma_x^2} \quad (2)$$

$$\epsilon_{part} = \frac{\sigma_y'^2 - \sigma_x'^2}{\sigma_y'^2 + \sigma_x'^2} = \frac{\sqrt{(\sigma_y^2 - \sigma_x^2)^2 + 4\sigma_{xy}^2}}{\sigma_y^2 + \sigma_x^2}. \quad (3)$$

Where $\sigma_y^2 = \langle y^2 \rangle - \langle y \rangle^2$, $\sigma_x^2 = \langle x^2 \rangle - \langle x \rangle^2$ are the variance in the shifted framework. It is clear from above definition that the ϵ_{std} really does not make much sense, since it is calculated for nucleus who's center may not located at $(-b/2, 0, 0)$ and $(b/2, 0, 0)$ due to fluctuations. Thus we strongly argue one should use ϵ_{rp} instead of ϵ_{std} .

The PHOBOS Glauber and the version that is modified to include BBC response have been checked into CVS area

/offline/analysis/glauber-phobos

³In the original calculation, Klaus assumed poisson distribution instead NBD.

All of the generated root files containing the distributions of the calculated quantities can be found under “/phenix/gh/data07/rwei/glauber/ppg098/new/simulationfile”.

For the Monte Carlo simulations the value $\sigma_{NN} = 42$ mb was used for the nucleon-nucleon cross section and the Wood-Saxon parameters for the density distribution of ^{197}Au was used:

- radius $R=6.38$ fm
- diffuseness $d=0.535$ fm

The nucleons were assumed to have no hard-core and the condition for nucleon-nucleon collision is that the inter-nucleon distance d should satisfy $\pi d^2 < \sigma_{NN}$. The input NBD parameter is $\mu = 4.00$ and $k = 1$. We call this set up as the “default settings”, which is also the default setting for PHENIX Glauber ⁴.

In Fig. 1, the left panel shows the Monte Carlo charge distribution obtained with the default parameter, and the right panel shows the BBC trigger efficiency as function of BBC charge. The overall efficiency is 94.2%, and efficiency loss becomes important when BBC charge < 100 . Centrality classes were defined from this distribution following the procedure discussed earlier. That is, the whole distribution range is truncated to give 93% efficiency (1.2% of lower BBC charged was discard as discussed earlier), which is then cut into its respective percentiles (0-5%, 5-10%, etc) and the corresponding values for the geometric quantities are calculated. The results from these calculations are shown in Table 1 below. This table not only include quantities calculated in previous PHENIX Glauber code, which include $\langle N_{part} \rangle$, $\langle N_{ncoll} \rangle$, $\langle b \rangle$, $\langle \epsilon_{std} \rangle$, but we also calculate three additional values $\langle \epsilon_{rp} \rangle$, $\langle \epsilon_{part} \rangle$ and average transverse size of the overlap region $\langle \bar{R} \rangle$.

As a cross check, we also chose $\mu = 4$ and $k = 1$ which directly gives the efficiency of 93% without the truncation (actually it gives 93.1% efficiency). We compare the associated Glauber results are compared with those from the default, and present the ratios in Figure 2. The difference between the two is less than 1% across all centrality bins.

The distributions of variables for different centralities are shown in Fig.3. It is interesting to notices that the distribution of all eccentricities quantities are quite broad, especially towards the peripheral collisions, in many cases, there are large fraction of events having negative values. This clearly indicates the effects of fluctuation is very big. However the value of participant eccentricity is always positive because it is calculated in the rotated frame where $\sigma_y^2 \geq \sigma_x^2$ is always satisfied.

Finally, the plots comparing the systematics for each parameter variation are shown in Figs. 5 - 8. The detailed discussion on how they are evaluated is presented in Section 3.4. Please refer to next section for details on the discussion of errors.

We want to discuss a little bit the meaning of \bar{R} because it is an interesting quantity that is used by PPG098. It's calculated event by event as [12]:

$$\frac{1}{\bar{R}^2} = \frac{1}{\langle x^2 - \langle x \rangle \rangle} + \frac{1}{\langle y^2 - \langle y \rangle \rangle} \equiv \frac{1}{\sigma_x^2} + \frac{1}{\sigma_y^2} \quad (4)$$

This definition is very similar to the harmonic mean (except a factor of $\sqrt{2}$ on \bar{R} is missing). It is a good quantity for characterizing the average of rate of change or pressure gradient. For an almond shaped overlap region, the value of \bar{R} is dominated by the size of the short direction

⁴this, plus disabling the re-adjustment of b , is the setting we used to produce the comparison in Appendix A

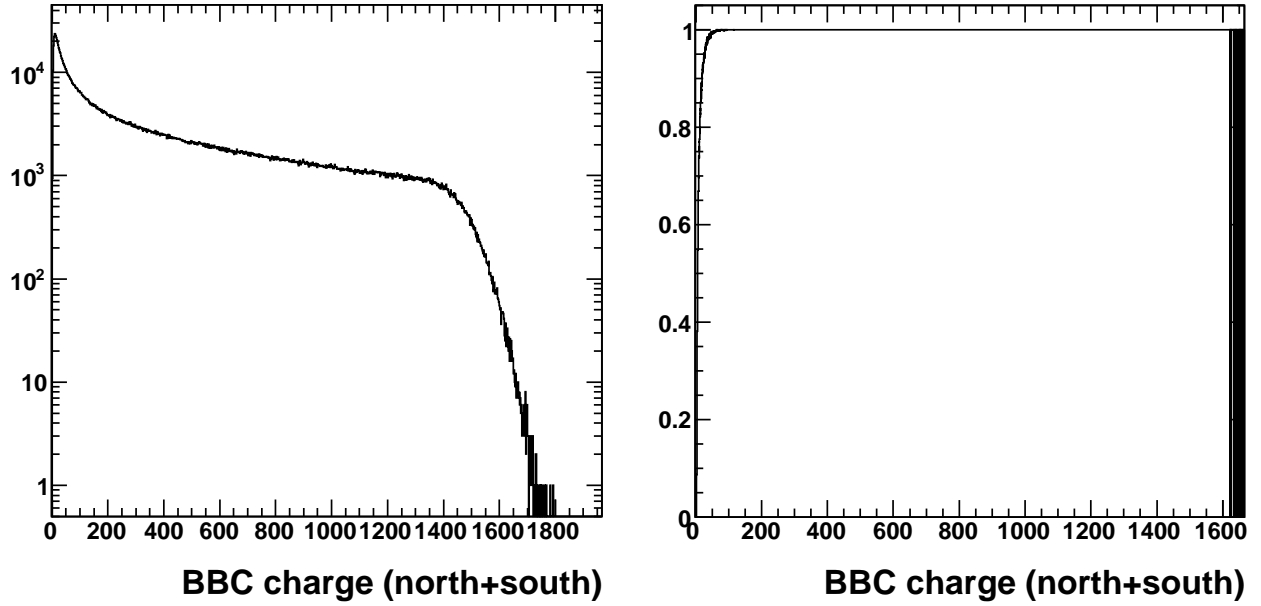


Figure 1: Left: Simulated BBC charge distribution. It is used to determine the centrality classes. Right: BBC trigger efficiency.

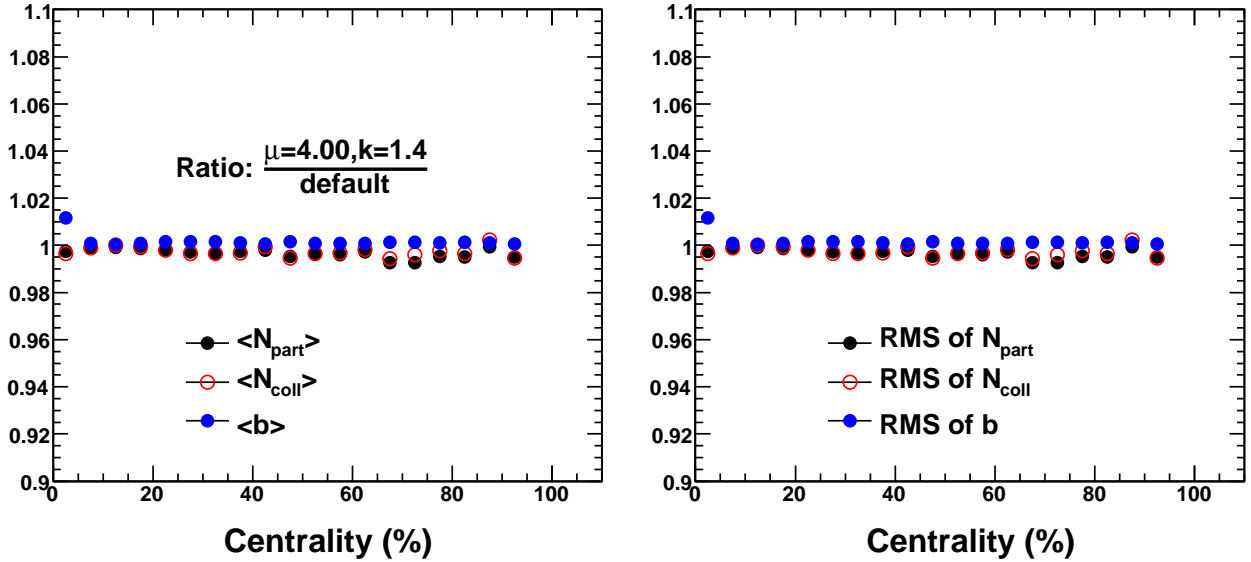


Figure 2: Ratio of the Mean value (left panel) and RMS value (right panel) Glauber quantities, N_{part} , N_{coll} and b , between those produced with $\mu = 4.00$ and $k = 1.4$ and those from default Table 1.

where the pressure gradient and flow is the largest. Thus this quantify was argued [12] to be suitable for flow study. One could imagine to define R differently such as geometrical mean, $\bar{R}^2 = \sqrt{\sigma_x^2 \sigma_y^2}$, or arithmetic mean $2\bar{R}^2 = \sigma_x^2 + \sigma_y^2$. These definitions were not explored here.

Finally we want to point out that the mean value of all the glauber quantities shown in Table 1 agrees with those calculated via PHENIX Glauber model by Klaus, but they are systematically higher then lower towards the peripheral collisions. Figure 4 shows the ratio

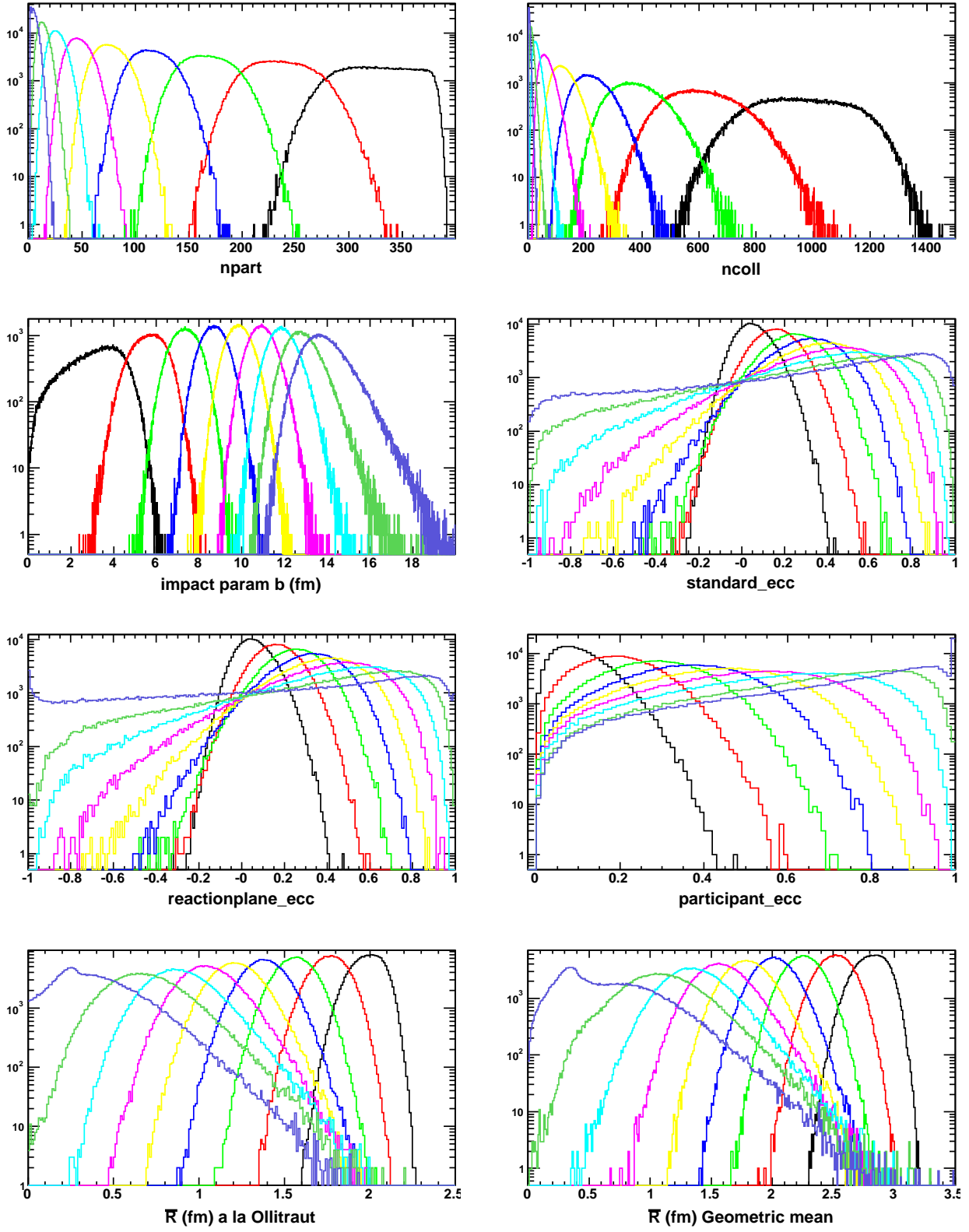


Figure 3: The distributions of variables (N_{part} , N_{coll} , impact parameter, three different eccentricities, transverse size a la $\frac{1}{\bar{R}^2} = \frac{1}{\sigma_x^2} + \frac{1}{\sigma_y^2}$, and $\bar{R}^2 = \sqrt{\sigma_x^2 \sigma_y^2}$) in 10 percent step centrality (last bin is 80-93%). Different color represents different centrality class. Note participant eccentricity is always positive definite.

Table 1: The average values and corresponding RMS values (in parenthesis) for Glauber quantities with default setting. NBD parameter is $\mu = 4.0$, $k = 1.4$ and $\alpha = 1$ (THIS IS THE DEFULAT)

Bin %	$\langle N_{\text{part}} \rangle$	$\langle N_{\text{coll}} \rangle$	$\langle b \rangle$	$\langle \epsilon_{\text{std}} \rangle$	$\langle \epsilon_{rp} \rangle$	$\langle \epsilon_{part} \rangle$	$\langle R \rangle$	$\langle T_{AB} \rangle$
	$\sigma_{N_{\text{part}}}$	$\sigma_{N_{\text{coll}}}$	σ_b	$\sigma_{\epsilon_{\text{std}}}$	$\sigma_{\epsilon_{rp}}$	$\sigma_{\epsilon_{part}}$	σ_R	$\sigma_{T_{AB}}$
0-5	350.8	1067	2.284	0.02635	0.02689	0.08342	2.041	25.4
	(20.38	109	0.9034	0.06469	0.06494	0.04556	0.06504	2.595)
5-10	301.7	857.8	3.949	0.08232	0.08384	0.1265	1.929	20.42
	(22.32	108.1	0.6888	0.07911	0.07946	0.06349	0.07668	2.573)
10-15	255.7	680.2	5.161	0.1356	0.1382	0.1754	1.815	16.19
	(20.07	92.96	0.5631	0.09041	0.09073	0.07748	0.08221	2.213)
15-20	216.4	538.7	6.13	0.1808	0.1845	0.2211	1.709	12.83
	(18	80.16	0.5076	0.1021	0.1024	0.08985	0.08819	1.909)
20-25	182.4	424.4	6.96	0.2202	0.2251	0.2636	1.61	10.11
	(16.25	68.67	0.4796	0.1146	0.1149	0.1008	0.09489	1.635)
25-30	152.7	330.9	7.705	0.2551	0.2614	0.3037	1.515	7.879
	(14.69	58.46	0.4666	0.1282	0.1281	0.1117	0.1019	1.392)
30-35	126.8	254.7	8.385	0.2849	0.2927	0.3408	1.426	6.065
	(13.18	49.11	0.4624	0.1428	0.1426	0.1225	0.1103	1.169)
35-40	104.2	193.1	9.014	0.31	0.3195	0.3752	1.339	4.599
	(11.81	40.61	0.4626	0.1608	0.1603	0.1347	0.1192	0.9668)
40-45	84.59	143.9	9.603	0.3319	0.3433	0.4088	1.258	3.425
	(10.56	33.04	0.4725	0.1788	0.1781	0.1455	0.1288	0.7867)
45-50	67.73	105.4	10.15	0.3489	0.3625	0.4413	1.178	2.511
	(9.368	26.46	0.486	0.2013	0.2004	0.1572	0.1396	0.6301)
50-55	53.16	75.22	10.69	0.3629	0.3793	0.4771	1.099	1.791
	(8.201	20.56	0.506	0.2269	0.2257	0.1682	0.1518	0.4896)
55-60	40.96	52.52	11.19	0.3713	0.3904	0.5136	1.02	1.251
	(7.103	15.62	0.5283	0.2579	0.2569	0.1791	0.1638	0.372)
60-65	30.77	35.67	11.69	0.3748	0.3969	0.553	0.9398	0.8494
	(6.097	11.6	0.5598	0.292	0.2925	0.1899	0.1787	0.2762)
65-70	22.64	23.77	12.16	0.3714	0.3948	0.5978	0.8548	0.566
	(5.157	8.442	0.6025	0.3339	0.3378	0.1992	0.1928	0.201)
70-75	16.14	15.37	12.63	0.3627	0.3842	0.6478	0.7558	0.3659
	(4.314	6.051	0.6631	0.3831	0.39	0.2045	0.2074	0.1441)
75-80	11.15	9.686	13.09	0.35	0.358	0.6949	0.6414	0.2306
	(3.514	4.275	0.7506	0.4344	0.444	0.2077	0.2201	0.1018)
80-85	7.43	5.875	13.57	0.3418	0.2934	0.7237	0.5087	0.1399
	(2.824	3.002	0.8504	0.4816	0.5052	0.2146	0.2302	0.07147)
85-90	4.761	3.395	14.05	0.3344	0.1395	0.7498	0.3601	0.08084
	(2.141	2.034	0.9737	0.5291	0.5876	0.2288	0.2198	0.04843)
90-93	3.23	2.065	14.44	0.3341	-0.04262	0.7956	0.2447	0.04918
	(1.436	1.29	1.037	0.5586	0.6328	0.236	0.1786	0.03071)

of the our default Glauber quantities to the previous official number based on Clock method. The error band is the systematic error from Klaus study. As one can see, the difference is less than 5% except the most two peripheral bins (80-93%), all within previously quoted systematic errors.

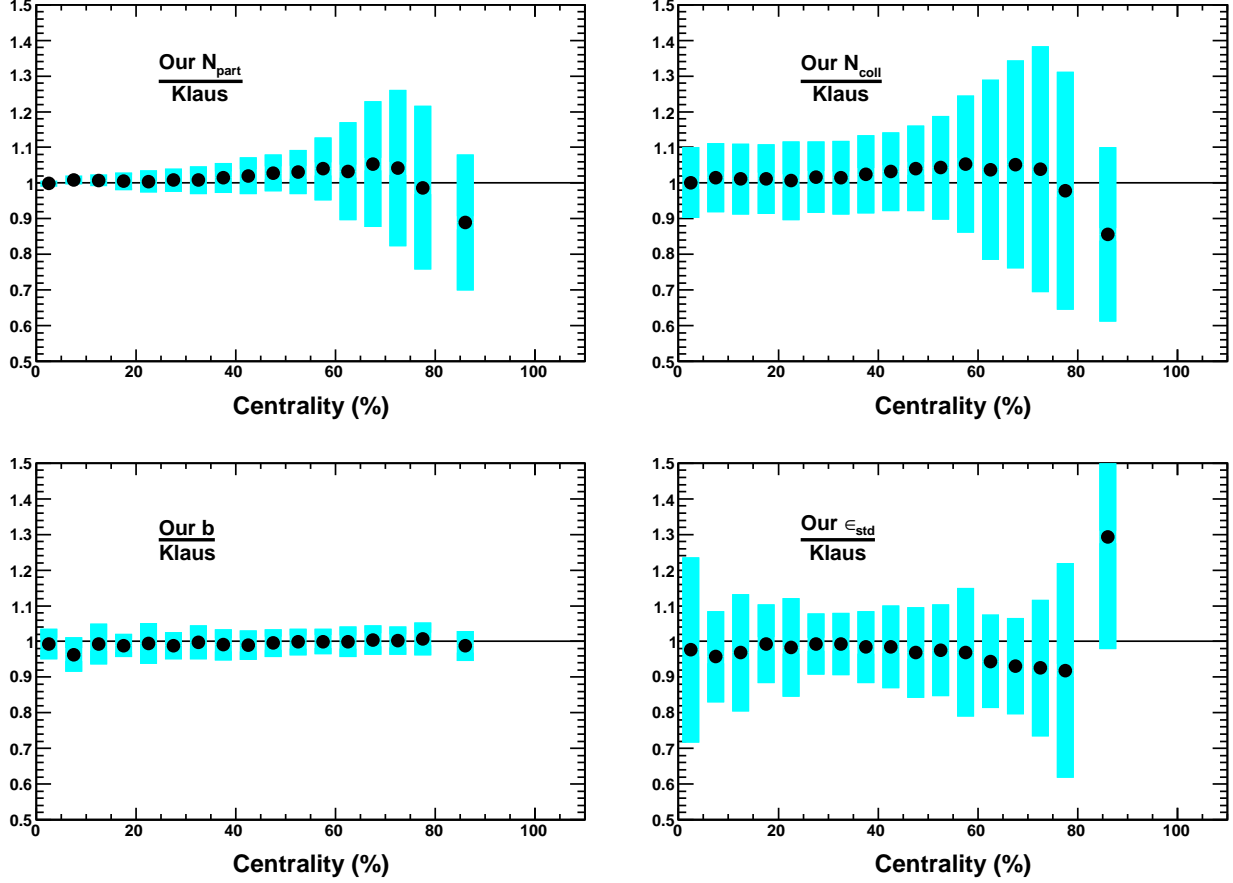


Figure 4: Ratio of the Glauber quantities (N_{part} , N_{coll} , b and ϵ_{std}) between RUN7 from Table 1 and Klaus' values. The light blue error bands is the corresponding systematic errors from the official web page.

To understand the origin for such difference, we need to pay attention to the difference in their definition and analysis procedures. According to analysis note 169 [9], Klaus' number were calculated on Feb.17 2003 or earlier. There are a number of changes which were not included back then

- The BBC response were calculated assuming poisson statistics. The mean of BBC hit per participant was chosen to reproduce the trigger efficiency of 92.2%. Since then, NBD distribution with parameters tuned to data is used. In current calculation, the BBC efficiency in the Glauber model is 94.2%.
- Previous Glauber model values were defined for clock method, i.e. both BBC and ZDC response were included. In current glauber model calculation, only BBC response is used. It was shown in An461 that the Clock method is prone to bigger fluctuations and systematic shift in the its mean values.

We believe that most of the difference is caused by the difference in the overall efficiency in the Glauber simulation.

3.4 Evaluation of systematic errors

In order to estimate the systematic errors for the calculated geometric quantities, the calculations were repeated for different settings of several model parameters etc, as summarized below. We try to repeat most the cross checks down by Klaus in AN169, in order to minimize any potential confusions. The list of checks we have done are the following:

- Change the cross section to 39mb; (default is 42mb)
- Change the cross section to 45mb;
- Change the Wood-Saxon function parameters $R=6.65\text{fm}$, $a=0.55\text{fm}$; (default: $R=6.38\text{fm}$, $a=0.535$)
- Change the Wood-Saxon function parameters $R=6.25\text{fm}$, $a=0.53\text{fm}$;
- In the default calculation nucleons are allowed to overlap. In this calculation nucleons are simulated with a hard core. The radius of the hard core was taken as PHOBOS's default value, such that the distance between the centers of two nucleons is always greater than $r = 0.4 \text{ fm}$.
- This uncertainty on minimum bias efficiency is assumed to be 93 ± 2 . This uncertainty is translated into an error of the extracted quantities. For this purpose the percentiles of the cross section in the simulation were modified by a fraction $2/93$, such that a slightly more central event sample was selected for each centrality class. N_{coll} is e.g. determined in the simulation for the 0-9.79% most central events instead of the 0-10% most central events.
- As in previous calculation, but a slightly less central event samples for each centrality class was selected. E.g. the 0-10.21% most central events instead of the 0-10% most central events were evaluated.
- μ , k was found to depends on the BBC z vertex, the difference between the using z dependent μ k and μ k fixed at the average value are evaluated and included as error (see Figure. 22).
- NBD with $\mu = 4.0$, $k = 1.0$ also gives 93% trigger efficiency, the difference of the resulting Glauber variable from default is evaluated (see Figure. 2).

The final systematic error of an extracted quantity for a given centrality class is the quadratic sum of all differences compared to the default calculation: $\epsilon_x = \sqrt{\sum_i (x_i - x_{default})^2}$, separately for those checks that produce systematically higher values and those produce systematically lower values, where x stands for extracted quantity. e.g. N_{coll} . Then the larger of the higher and lower systematic errors are used as the final systematic errors. Fig.5-Fig.12 show the comparisons of these quantities.

The final numbers with the associated systematic errors are documented in Table 2-4, we have combined 80-85%, 85-90% and 90-93% into a single bin to be consistent with previous study.

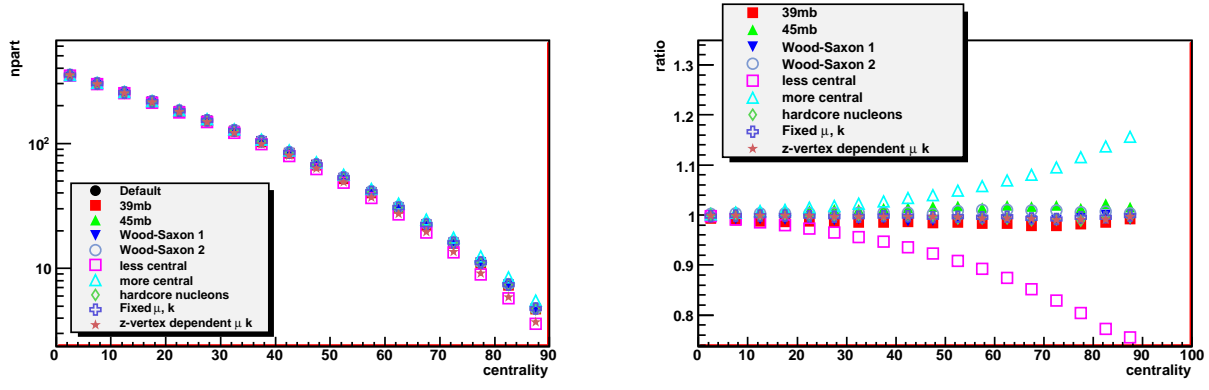


Figure 5: Comparison of $\langle N_{\text{part}} \rangle$ values. The right panel shows the ratio to the default.

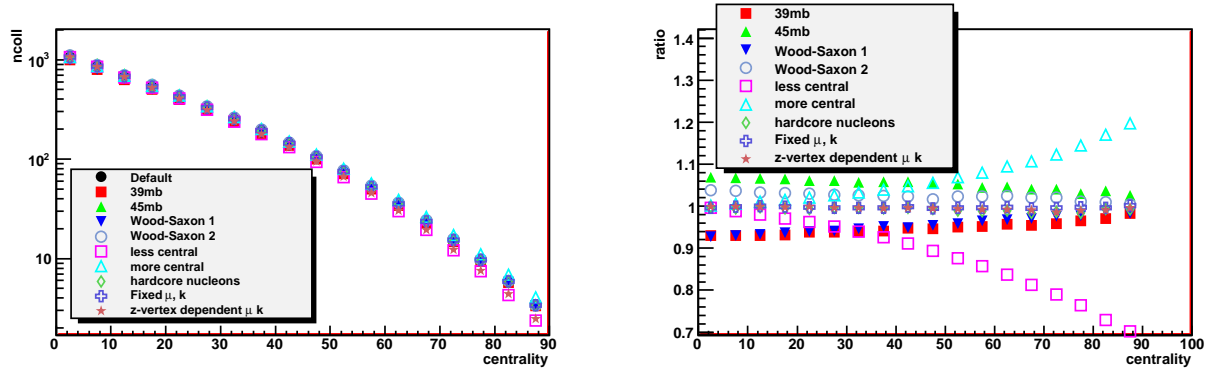


Figure 6: Comparison of $\langle N_{\text{coll}} \rangle$ values. The right panel shows the ratio to the default.

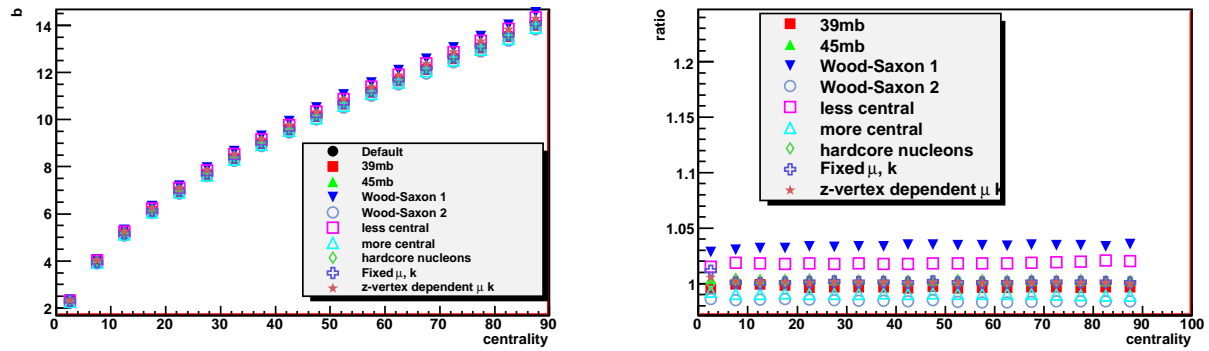


Figure 7: Comparison of the $\langle b \rangle$ (impact parameter) values. The right panel shows the ratio to the default.

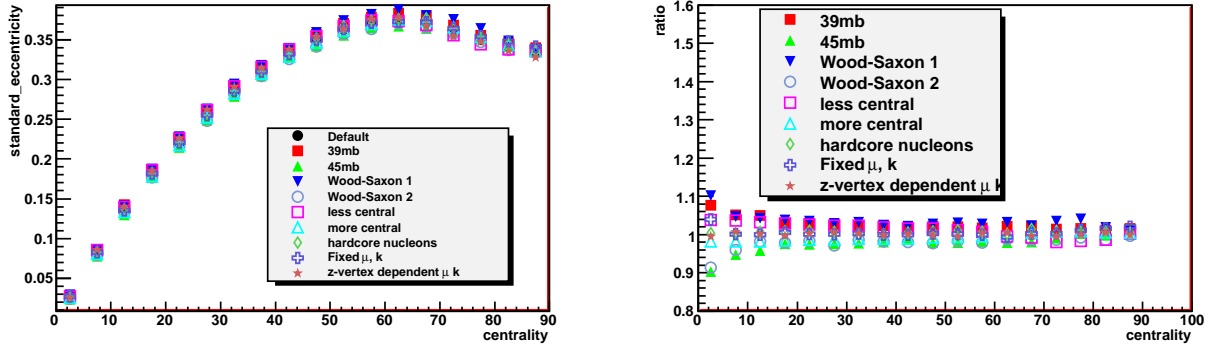


Figure 8: Comparison of $\langle \epsilon_{std} \rangle$ (standard eccentricity) values. The right panel shows the ratio to the default.

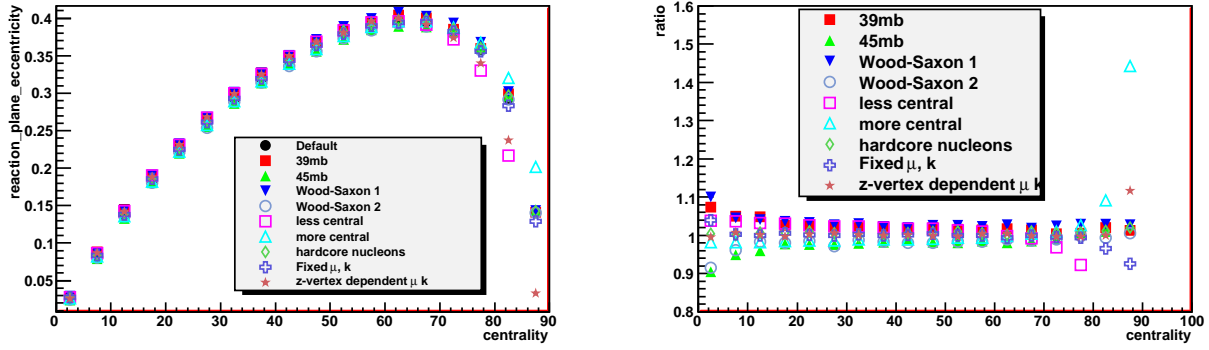


Figure 9: Comparison of $\langle \epsilon_{rp} \rangle$ (reaction plane eccentricity) values. The right panel shows the ratio to the default.

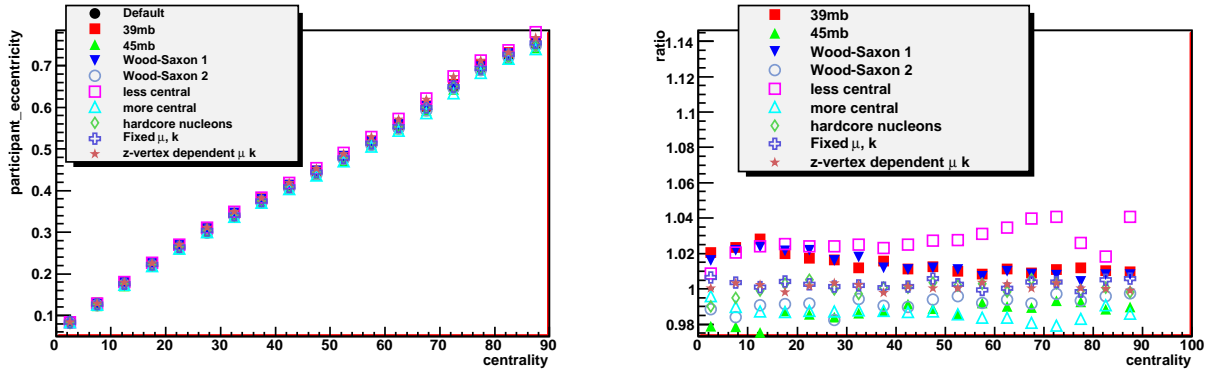
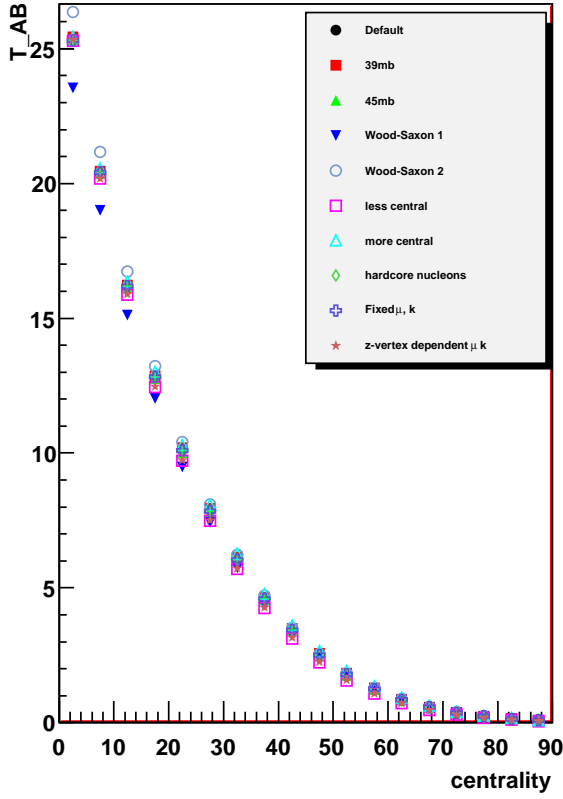


Figure 10: Comparison of the $\langle \epsilon_{part} \rangle$ (participant eccentricity) values. The right panel shows the ratio to the default.

hcent_0_7



hframe

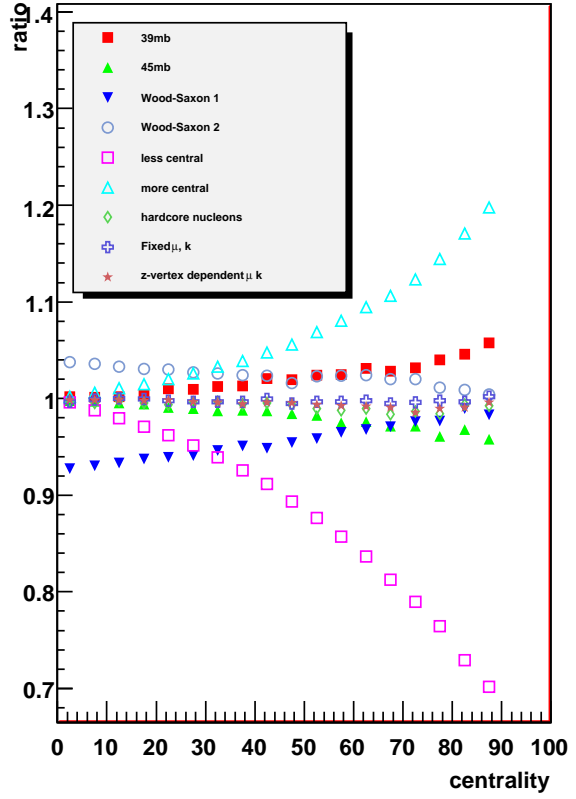


Figure 11: Comparison of $\langle T_{AB} \rangle$ values. The right panel shows the ratio to the default. Since $\langle T_{AB} \rangle = \langle N_{coll} \rangle / \sigma_{nn}$, most of the errors is of the same magnitude as that for $\langle N_{coll} \rangle$.

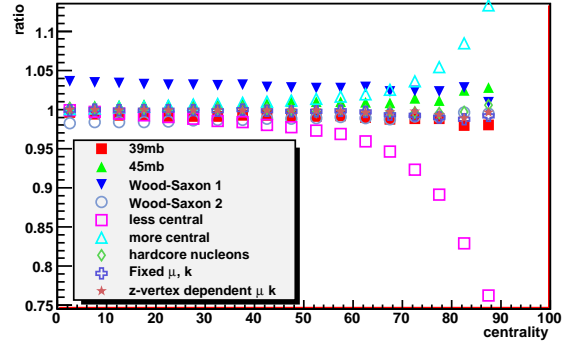
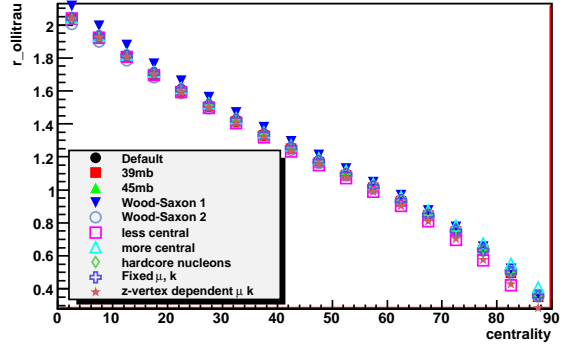


Figure 12: Comparison of $\langle \bar{R} \rangle$ (transverse size) values. The right panel shows the ratio to the default.

Table 2: Parameters table with systematic errors (in parenthesis) in 5 percent step.

Bin %	$\langle N_{\text{part}} \rangle$ $S.E_{N_{\text{part}}}$	$\langle N_{\text{coll}} \rangle$ $S.E_{N_{\text{coll}}}$	$\langle b \rangle$ $S.E_b$	$\langle \epsilon_{\text{std}} \rangle$ $S.E_{\epsilon_{\text{std}}}$	$\langle \epsilon_{rp} \rangle$ $S.E_{\epsilon_{rp}}$	$\langle \epsilon_{part} \rangle$ $S.E_{\epsilon_{part}}$	$\langle R \rangle$ $S.E_{\bar{R}}$	$\langle T_{AB} \rangle$ $S.E_{T_{AB}}$
0-5	350.8 (3.092)	1067 107.7	2.284 0.0746	0.02635 0.003517	0.02689 0.00351	0.08342 0.002295	2.041 0.07485	25.4 1.855)
5-10	301.7 (4.665)	857.8 85.45	3.949 0.1421	0.08232 0.00647	0.08384 0.006449	0.1265 0.004796	1.929 0.06779	20.42 1.446)
10-15	255.7 (5.426)	680.2 67.26	5.161 0.1923	0.1356 0.009927	0.1382 0.009885	0.1754 0.007756	1.815 0.06217	16.19 1.136)
15-20	216.4 (5.619)	538.7 52.39	6.13 0.2258	0.1808 0.01019	0.1845 0.01022	0.2211 0.008584	1.709 0.05654	12.83 0.8909)
20-25	182.4 (5.743)	424.4 40.37	6.96 0.2666	0.2202 0.01173	0.2251 0.01163	0.2636 0.009796	1.61 0.05234	10.11 0.7354)
25-30	152.7 (5.903)	330.9 32.68	7.705 0.2919	0.2551 0.01181	0.2614 0.01146	0.3037 0.01014	1.515 0.04991	7.879 0.6079)
30-35	126.8 (5.945)	254.7 25.78	8.385 0.3193	0.2849 0.01299	0.2927 0.01285	0.3408 0.01128	1.426 0.04706	6.065 0.5012)
35-40	104.2 (5.758)	193.1 20.71	9.014 0.3426	0.31 0.0121	0.3195 0.01222	0.3752 0.01141	1.339 0.04557	4.599 0.4141)
40-45	84.59 (5.639)	143.9 16.51	9.603 0.3798	0.3319 0.01113	0.3433 0.01092	0.4088 0.01208	1.258 0.03998	3.425 0.353)
45-50	67.73 (5.405)	105.4 13.5	10.15 0.4027	0.3489 0.01401	0.3625 0.01404	0.4414 0.01434	1.178 0.03776	2.511 0.2945)
50-55	53.16 (4.96)	75.22 10.53	10.69 0.418	0.3629 0.0143	0.3793 0.01339	0.4771 0.01493	1.099 0.03541	1.791 0.2367)
55-60	40.96 (4.478)	52.52 8.164	11.19 0.4369	0.3713 0.013	0.3904 0.01146	0.5136 0.01696	1.02 0.03456	1.251 0.1875)
60-65	30.77 (3.911)	35.67 6.135	11.69 0.4549	0.3748 0.01494	0.3969 0.01288	0.553 0.02084	0.9398 0.04041	0.8494 0.143)
65-70	22.64 (3.406)	23.77 4.658	12.16 0.4844	0.3714 0.01331	0.3948 0.0106	0.5978 0.02519	0.8548 0.04826	0.566 0.1091)
70-75	16.14 (2.791)	15.37 3.323	12.63 0.5007	0.3627 0.01434	0.3842 0.01311	0.6478 0.02782	0.7558 0.05903	0.3659 0.07832)
75-80	11.15 (2.194)	9.686 2.323	13.09 0.5223	0.35 0.01565	0.358 0.02758	0.6949 0.02006	0.6414 0.07038	0.2306 0.05548)
80-93	5.601 (0.8102)	4.193 0.761	13.92 0.5059	0.3375 0.00725	0.1703 0.04624	0.7451 0.01317	0.4012 0.04566	0.09984 0.01837)

Table 3: Parameters table with systematic errors (in parenthesis) in 10 percent step.

Bin %	$\langle N_{\text{part}} \rangle$ $S.E_{N_{\text{part}}}$	$\langle N_{\text{coll}} \rangle$ $S.E_{N_{\text{coll}}}$	$\langle b \rangle$ $S.E_b$	$\langle \epsilon_{\text{std}} \rangle$ $S.E_{\epsilon_{\text{std}}}$	$\langle \epsilon_{rp} \rangle$ $S.E_{\epsilon_{rp}}$	$\langle \epsilon_{part} \rangle$ $S.E_{\epsilon_{part}}$	$\langle R \rangle$ $S.E_{\bar{R}}$	$\langle T_{AB} \rangle$ $S.E_{T_{AB}}$
0-10	325.8 (3.81)	960.2 (96.14)	3.132 (0.1079)	0.05487 (0.004948)	0.05591 (0.004928)	0.1054 (0.003514)	1.984 (0.07124)	22.86 (1.642)
10-20	236.1 (5.517)	609.5 (59.81)	5.645 (0.2092)	0.1582 (0.01)	0.1613 (0.009999)	0.1983 (0.008148)	1.762 (0.0593)	14.51 (1.012)
20-30	167.6 (5.811)	377.6 (36.39)	7.333 (0.2783)	0.2377 (0.01173)	0.2432 (0.0115)	0.2837 (0.009891)	1.563 (0.05125)	8.991 (0.6677)
30-40	115.5 (5.841)	223.9 (23.2)	8.699 (0.3311)	0.2975 (0.01252)	0.3061 (0.01248)	0.358 (0.01127)	1.383 (0.04626)	5.332 (0.4564)
40-50	76.15 (5.502)	124.6 (14.94)	9.877 (0.3908)	0.3404 (0.01254)	0.3529 (0.01244)	0.4251 (0.01316)	1.218 (0.03889)	2.968 (0.322)
50-60	47.07 (4.726)	63.9 (9.359)	10.94 (0.4278)	0.3671 (0.01364)	0.3848 (0.01243)	0.4953 (0.01593)	1.06 (0.03448)	1.521 (0.2123)
60-70	26.72 (3.669)	29.75 (5.41)	11.92 (0.4699)	0.3731 (0.0138)	0.3959 (0.01148)	0.5753 (0.02294)	0.8975 (0.04445)	0.7083 (0.1264)
70-80	13.67 (2.492)	12.55 (2.822)	12.86 (0.5104)	0.3564 (0.01499)	0.3712 (0.01993)	0.6711 (0.0238)	0.6991 (0.06457)	0.2988 (0.06695)
80-90	6.153 (1.359)	4.688 (1.252)	13.8 (0.5484)	0.3383 (0.007611)	0.2198 (0.09558)	0.7357 (0.02097)	0.4376 (0.08141)	0.1116 (0.02998)

Table 4: Parameters table with systematic errors (in parenthesis) in 20 percent step.

Bin %	$\langle N_{\text{part}} \rangle$ $S.E_{N_{\text{part}}}$	$\langle N_{\text{coll}} \rangle$ $S.E_{N_{\text{coll}}}$	$\langle b \rangle$ $S.E_b$	$\langle \epsilon_{\text{std}} \rangle$ $S.E_{\epsilon_{\text{std}}}$	$\langle \epsilon_{rp} \rangle$ $S.E_{\epsilon_{rp}}$	$\langle \epsilon_{part} \rangle$ $S.E_{\epsilon_{part}}$	$\langle R \rangle$ $S.E_{\bar{R}}$	$\langle T_{AB} \rangle$ $S.E_{T_{AB}}$
0-20	280.5 (4.58)	783.2 (77.47)	4.401 (0.1584)	0.107 (0.007469)	0.1091 (0.007455)	0.1523 (0.005823)	1.872 (0.06521)	18.65 (1.312)
20-40	141.5 (5.817)	300.8 (29.64)	8.016 (0.3049)	0.2676 (0.01211)	0.2747 (0.01198)	0.3208 (0.01058)	1.473 (0.04866)	7.162 (0.5571)
40-60	61.6 (5.08)	94.23 (12.03)	10.41 (0.4089)	0.3537 (0.013)	0.3689 (0.01235)	0.4602 (0.01444)	1.139 (0.0366)	2.244 (0.2648)
60-80	20.2 (3.017)	21.16 (4.034)	12.39 (0.4877)	0.3648 (0.01422)	0.3835 (0.01175)	0.6232 (0.0228)	0.7983 (0.05314)	0.5037 (0.0949)

4 Appendix A: Comparison between PHENIX and PHOBOS Glauber MC

The glauber calculation is rather straightforward. The numbers of line of code is about 1100 for the Phobos version and 1800 for the PHENIX version. So it is not difficult to find out that the logic of the codes are very similar between the two. But in any case, in order to ensure the consistency with previous glauber calculation, we need to make sure the two set of codes produce identical results when the steering parameters are set to be the same.

To do this comparison, we have run both Glauber codes using the PHENIX default setup ($R=6.38\text{fm}$, $d=0.535$, $\sigma_{nn}=42\text{mb}$, no hard-core for nucleons). The corresponding setup file can be found in the CVS directory. About 2 million events were generated for impact parameter from 0-15 fm in each cases. To avoid the additional complications from BBC trigger efficiency, we keep all events and slice them into percentiles according to the impact parameter.

Figure 13-Figure 15 compare important parameters, N_{coll} , N_{part} and ecc_{std} , between the two set of codes. Clearly the differences for central are typically less than 1%.

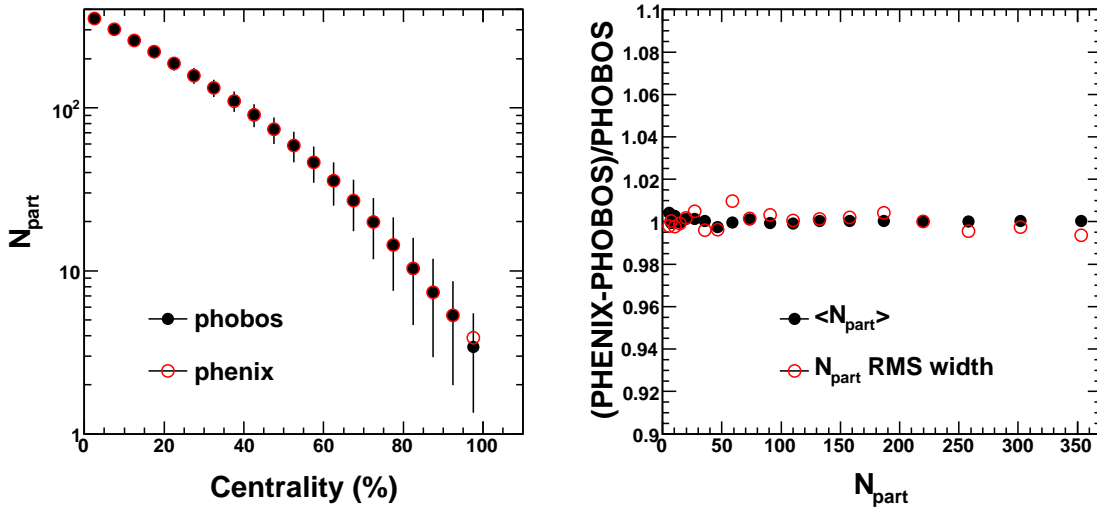


Figure 13: Comparison of the PHENIX and PHOBOS Glauber without detector response. (left) The $\langle N_{part} \rangle$ (points) and RMS (error bar) value as function of percentile (in 5% steps) defined by impact parameter; (right) the ratio of $\langle N_{part} \rangle$ and ratio of RMS width as function of $\langle N_{part} \rangle$.

There is a small caveat, on our first try, we actually found a small difference between the outputs from the two glauber codes. We dig into the PHOBOS code and found the following piece of code in the ThrowNucleons routine(right figure), which distribute the nucleons in the nucleus.

This code reshift the all nucleons by their average position such that its center-of-mass of the nucleons sits at $(\pm b/2, 0, 0)$. By doing this, the impact parameter is defined as the

```
if(1) { // set the centre-of-mass to be at zero (+xshift)
    sumx = sumx/fN;
    sumy = sumy/fN;
    sumz = sumz/fN;
    for (Int t i = 0; i<fN; i++) {
        TGlaueNucleon *nucleon=(TGlaueNucleon*)(fNucleons->At(i));
        nucleon->SetXYZ(nucleon->GetX()-sumx-xshift,
                        nucleon->GetY()-sumy,
                        nucleon->GetZ()-sumz);
    }
}
```

Figure 16: code from PHOBOS

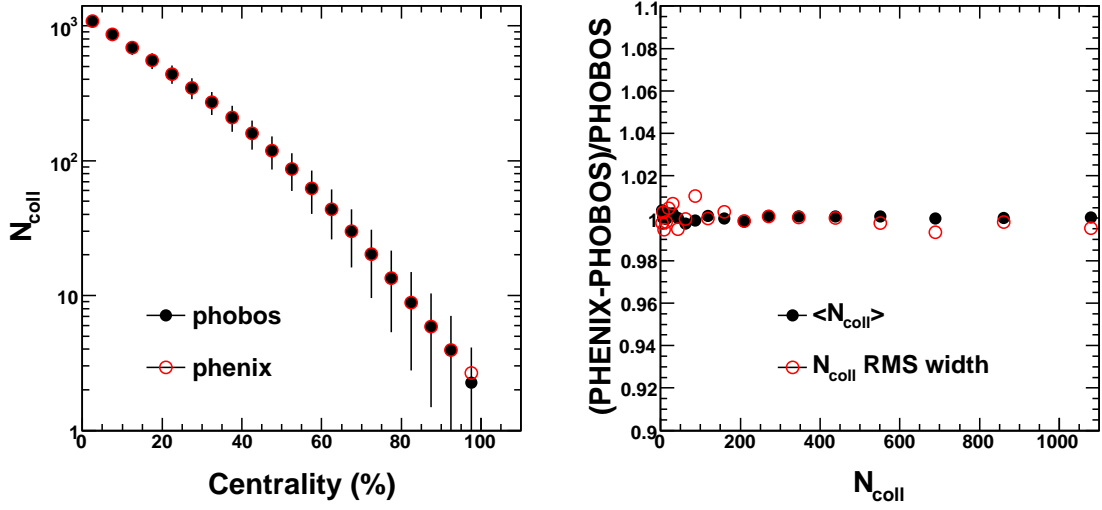


Figure 14: Comparison of the PHENIX and PHOBOS Glauber without detector response. (left) The $\langle N_{coll} \rangle$ (points) and RMS (error bar) value as function of percentile (in 5% steps) defined by impact parameter; (right) the ratio of $\langle N_{coll} \rangle$ and ratio of RMS width as function of $\langle N_{coll} \rangle$.

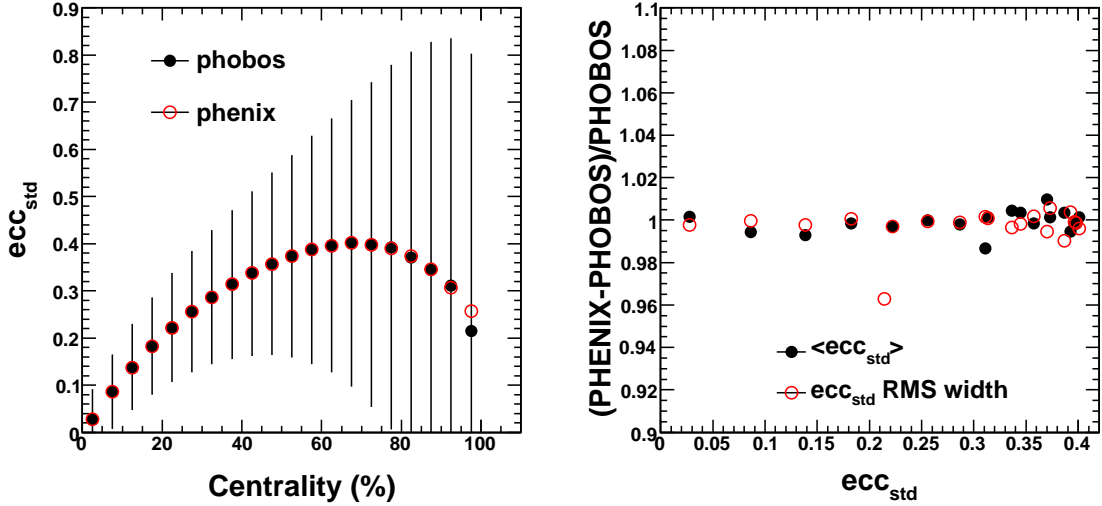


Figure 15: Comparison of the PHENIX and PHOBOS Glauber without detector response. (left) The $\langle ecc_{std} \rangle$ (points) and RMS (error bar) value as function of percentile (in 5% steps) defined by impact parameter; (right) the ratio of $\langle ecc_{std} \rangle$ and ratio of RMS width as function of $\langle ecc_{std} \rangle$. The difference for 95-100% bin is somewhat larger, but this is most peripheral bin, where the intrinsic fluctuation is big.

distance between the center-of-mass between the two nucleus. In PHENIX glauber, the center of the nucleus is given before the position of all the nucleons are determined. However because of the intrinsic fluctuation, the real center determined by all thrown nucleons clearly will be different, and the initial central position lost its meaning. We believe impact parameter defined by PHOBOS is a more physical definition.

For the cross check shown in Figure 13-Figure 15, we have disabled this piece of code for

proper comparison. What the code does is that it removes the unphysical smearing of the impact parameter. This smearing, such as in PHENIX Glauber, leads to artificial broadening of the distribution of N_{coll} and N_{part} when event classes are defined by impact parameter as shown in Figure 17. This broadening is rather large (40%) for mid-central bins, but it does not affect the mean values too much (on the order of 2%). One can imagine, this code should not affect the relation between BBC_{Charge} and N_{coll} , N_{part} , since their correlations are unchanged by this recentering procedure. Our points are illustrated by Figure., where we have enabled this piece of code, and we define our centrality by slicing on N_{part} . Clearly, the relation between N_{coll} and N_{part} are unchanged, but its relation to impacts parameters are different, especially the RMS width. We also notice that the standard eccentricity is sensitive to the additional fluctuation in impact parameter.

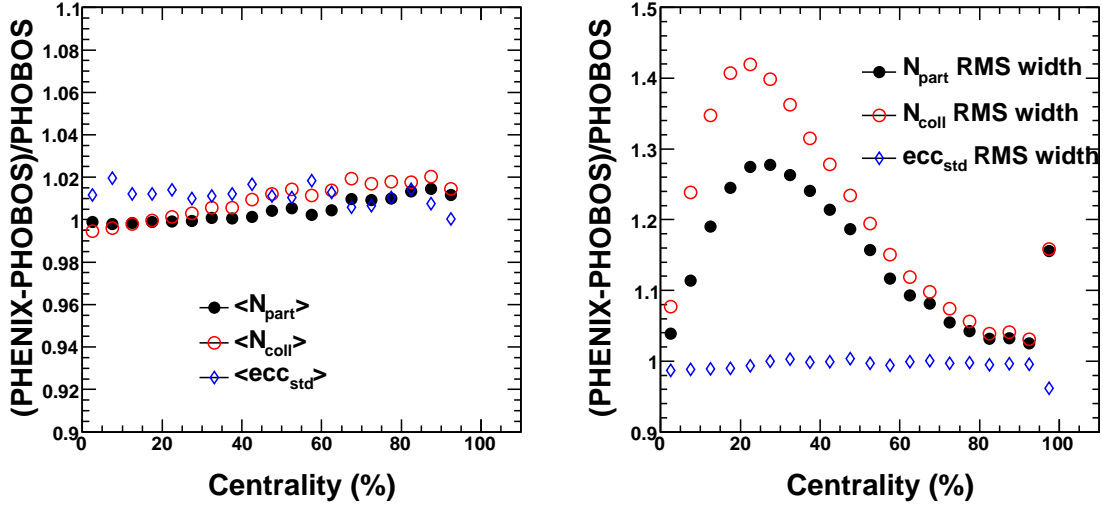


Figure 17: Comparison of the PHENIX and PHOBOS Glauber without detector response. The PHOBOS glauber recenter the nucleus using the center-of-mass of all nucleons, while PHENIX code does not. (left) Ratios of mean values of N_{part} , N_{coll} and ecc_{std} as function of percentile (in 5% steps) defined by impact parameter; (right) Ratios of RMS values of N_{part} , N_{coll} and ecc_{std} as function of percentile.

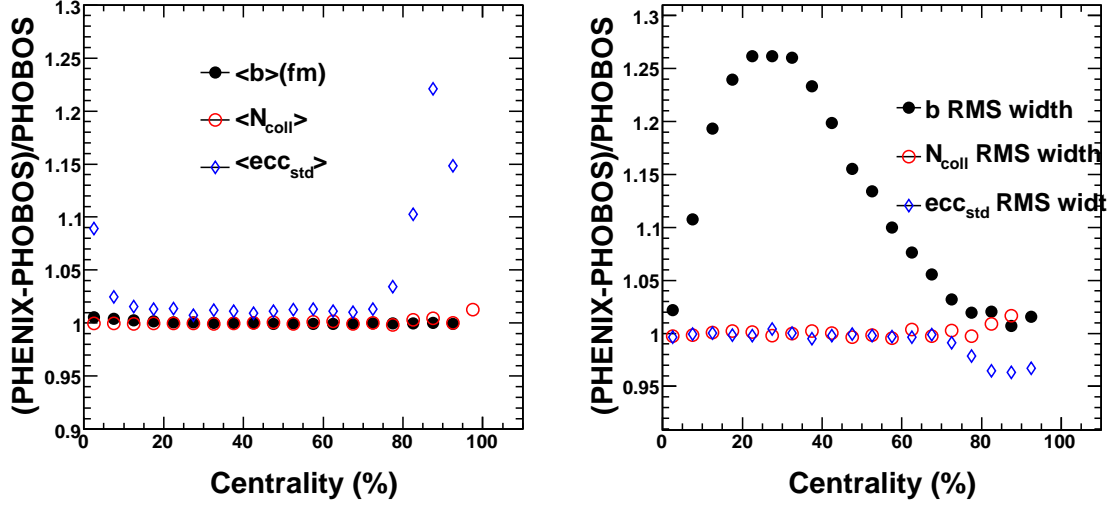


Figure 18: Comparison of the PHENIX and PHOBOS Glauber without detector response. The PHOBOS glauber recenter the nucleus using the center-of-mass of all nucleons, while PHENIX code does not. (left) Ratios of mean values of N_{part} , N_{coll} and ecc_{std} as function of percentile (in 5% steps) defined by N_{part} ; (right) Ratios of RMS values of N_{part} , N_{coll} and ecc_{std} as function of percentile.

5 Appendix B: Data driven NBD and its dependence on bbc z vertex

In analysis note 645, Sasha Milov found the value of μ and k depends on the BBC z vertex. As example, we show in Fig.19 the fit to BBC south (left panel) for the vertex selection $z_{vert} = 23$ cm. The ratio of the data to fit, shown in the right panel of Fig.19, is the minimum bias trigger efficiency plotted as a function of N_{hits} in the BBC. Fig.20 shows a reproduction (ie. taken from AN645) of the vertex dependence of μ (left panel) and k (right panel).

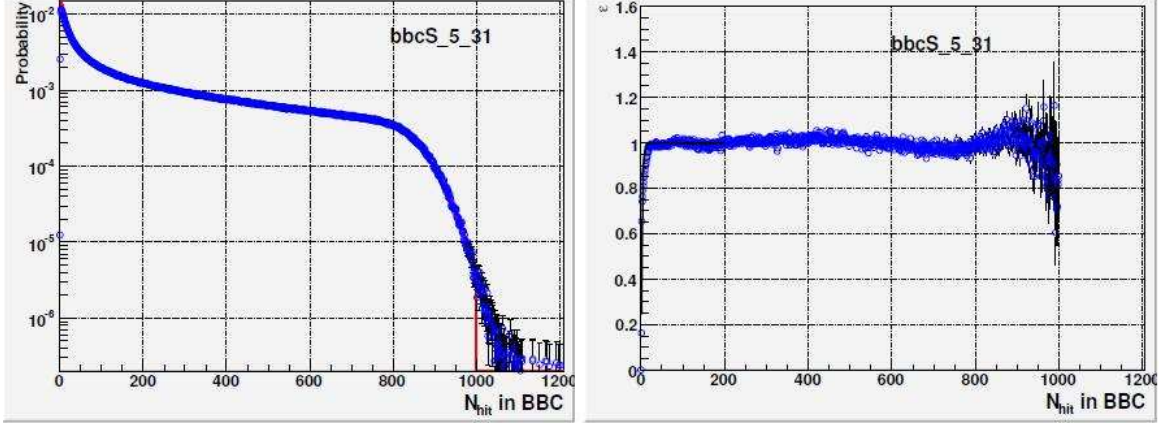


Figure 19: Left panel: BBC south distribution of the number of hits (blue) fitted to the NBD+Glauber (red). Right panel: Trigger efficiency vs. number of hits in the BBC.

To quantify the effects of the vertex dependence of Glauber parameters on the calculated Glauber variables. We run the Glauber code in two modes. In the first mode, we take into account the z vertex dependence of the μ and k separately for north and south BBCs. For each event, we randomly generate z-vertex from a parameterization of the real data as shown Figure 21. We then read off the corresponding μ and k parameter separately for BBC north and BBC south from Figure 20. We then generate the BBC charge in the usual way. In the second mode, we simply assume a fixed value of $\mu = 5$ and $k = 1.6$ independent on the vertex for both north and south BBC. This value of μ and k were simply the average values from Figure 20 weighted by the actual BBC z vertex distribution from Figure 21. We then plot the ratio of the N_{part} and N_{coll} as function of centrality percentile in Figure 22. As one can see, the difference on the calculated Glauber quantities is less than 1%. So the effects due to the z vertex dependence of μ and k is small and can be neglected.

The NBD parameters from RUN7 based on An645 is on the edge of the previously quoted systematic errors. As a consistency check we also looked at the use the NBD parameters ($\mu = 3.99$ and $k = 1.4$) from An461 based on RUN4 study but no z vertex dependence is included. This parameter gives a trigger efficiency of 94.5%, still on the high side but it is well within the systematic errors.

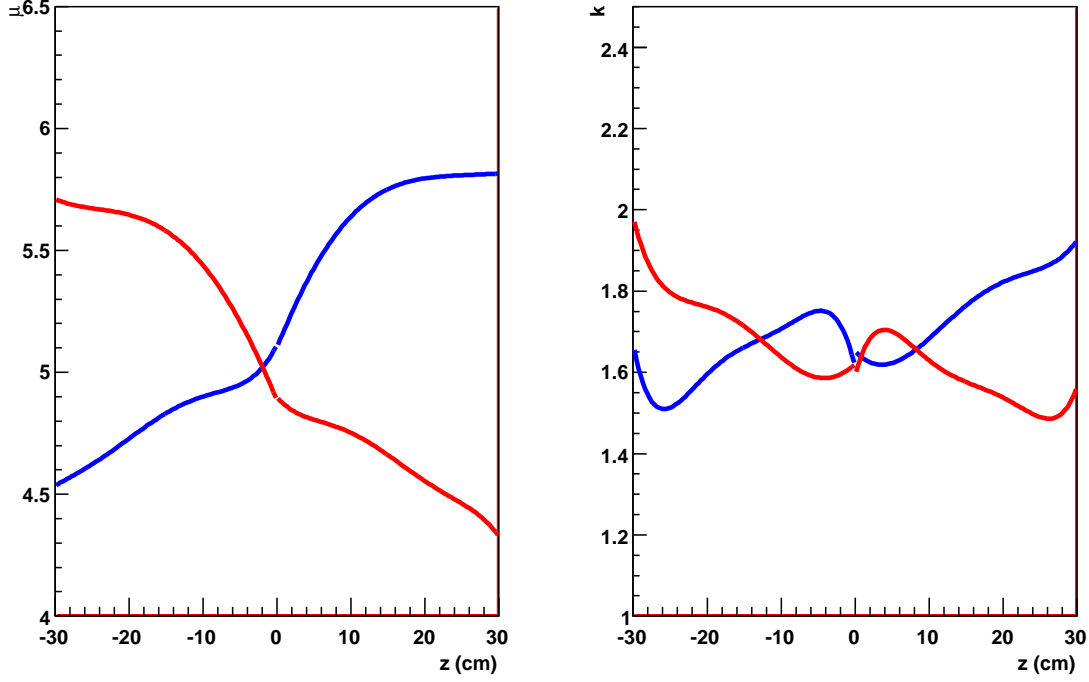


Figure 20: NBD parameters (μ and k) as function of the vertex z . The blue curve show the values for BBC north while the red curve show the values for BBC south. The data for this figure is taken from Fig. 5 in An645.

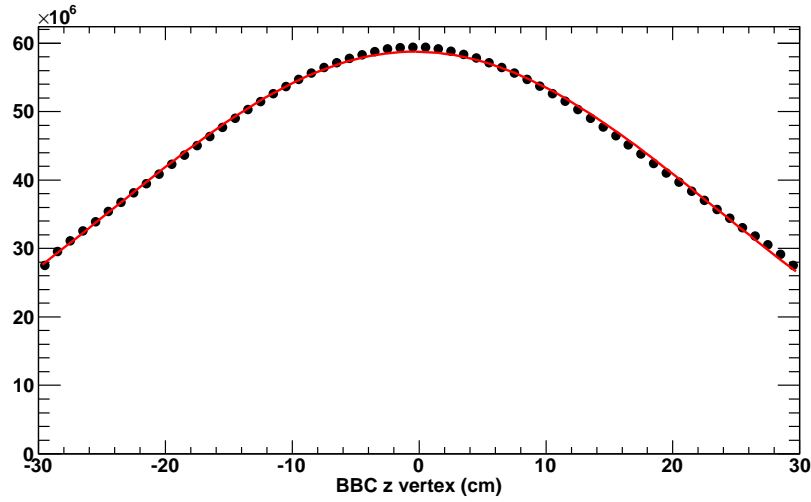


Figure 21: The BBC z vertex distribution and a gaussian parameterization based on 2.8 Billion RUN7 events.

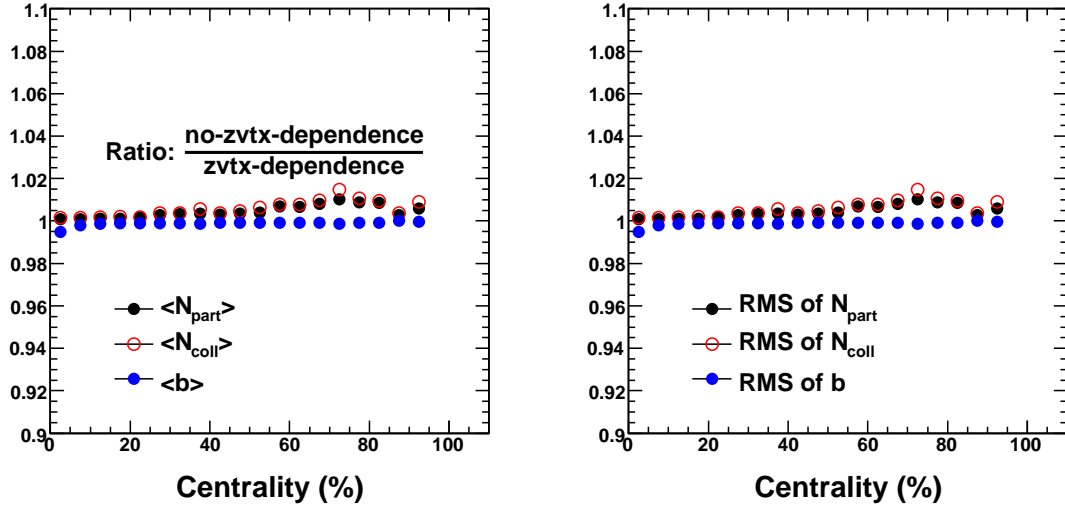


Figure 22: Ratio of the calculated mean values (left panel) and RMS values (right panel) as function of bbc percentile between without considering vertex dependence and with vertex dependence.

6 Appendix C: Participant eccentricity a la PHOBOS

As indicated earlier, we have used the PHOBOS Glauber Monte Carlo code for our evaluations. Since the participant eccentricity is important to PPG098 we have excerpted the description, given in Ref. [11], of the procedure implemented in the PHOBOS Glauber Monte Carlo for eccentricity evaluations.

< snip >

The spatial anisotropy of the interaction region in the transverse plane (in the following as throughout the paper given by the x - and y -axes) is commonly called “eccentricity” and denoted with the symbol ϵ . It has been introduced in [13] (called “deformation”, symbol δ) and in [14] (called “spatial asymmetry”, symbol α_x), while the basic idea of a dimensionless *momentum-based* anisotropy parameter (symbol α) originates from [15]. In its most basic formulation, the eccentricity definition reads

$$\epsilon = \frac{R_y^2 - R_x^2}{R_y^2 + R_x^2} \quad (5)$$

where R_x^2 and R_y^2 characterize the size of the source in the x - and y -direction, respectively. Note that this definition allows positive and negative values, $-1 \leq \epsilon \leq 1$. It is related, but not identical, to the geometrical definition of the eccentricity of an ellipse. In this appendix, we will summarize the most important definitions of eccentricity.

6.1 Standard Eccentricity

Prior to our work [16], it has been common practice to use smooth, event-averaged initial conditions, for which the initial spatial asymmetry in the transverse plane has typically been given by the “standard” eccentricity

$$\epsilon_s = \frac{\langle y^2 \rangle - \langle x^2 \rangle}{\langle y^2 \rangle + \langle x^2 \rangle} \quad (6)$$

where $\langle x^2 \rangle$ and $\langle y^2 \rangle$ are the second moments of the (typically participant-weighted) ensemble-averaged nucleon distribution in the x - and y -direction, respectively. We follow the notation introduced by Bhalerao & Ollitrault in [17], where $\langle \dots \rangle$ denotes an average taken over many events (ensemble average), while $\{ \dots \}$ stands for an average (over participants) in a single event (sample average).

6.2 Participant Eccentricity

The “participant” eccentricity expresses the overlap eccentricity in the rotated (“participant”) frame (see Fig. 23), denoted by x' and y' , which for a given event maximizes $\sigma_{y'}$ and minimizes $\sigma_{x'}$. In principle, the overlap zone will also be shifted with respect to the reaction plane frame, but this shift has no impact on the eccentricity. Generally, the second moments of the position distribution in the nuclear reaction plane (or MC) frame are described by the covariance matrix,

$$\Sigma = \begin{pmatrix} \sigma_x^2 & \sigma_{xy} \\ \sigma_{xy} & \sigma_y^2 \end{pmatrix} \quad (7)$$

where σ_x^2 , σ_y^2 and $\sigma_{xy} = \{xy\} - \{x\}\{y\}$ are the per-event (co-)variances of the underlying (typically participant weighted) nucleon distribution in the transverse plane, given in the original

frame. The participant frame corresponds to the frame in which Σ is diagonal. Since Σ is a real symmetric matrix, its diagonalization can be accomplished by finding the eigenvalues λ that satisfy $\det(\Sigma - \lambda I) = 0$, leading to a second order polynomial in λ with two solutions:

$$\lambda^{\pm} = \frac{1}{2} \left(\sigma_y^2 + \sigma_x^2 \pm \sqrt{(\sigma_y^2 - \sigma_x^2)^2 + 4\sigma_{xy}^2} \right). \quad (8)$$

These two values of λ correspond to $\sigma_x'^2$ and $\sigma_y'^2$ with the larger value (λ^+) corresponding to the y' and the smaller value (λ^-) to the x' direction, by definition. This leads to the expression for the participant eccentricity [16, 18],

$$\epsilon_{\text{part}} = \frac{\sigma_y'^2 - \sigma_x'^2}{\sigma_y'^2 + \sigma_x'^2} = \frac{\sqrt{(\sigma_y^2 - \sigma_x^2)^2 + 4\sigma_{xy}^2}}{\sigma_y^2 + \sigma_x^2}. \quad (9)$$

Like ϵ_{RP} , the participant eccentricity is defined on an event-wise basis, however in contrast to the previous definitions of the eccentricity, it is non-negative, covering the range $0 \leq \epsilon_{\text{part}} \leq 1$ by construction. The participant frame is tilted event-by-event by an angle of Ψ_{part} with respect to the reaction plane, where

$$\tan \Psi_{\text{part}} = \frac{\sigma_{xy}}{\sigma_y^2 - \lambda^-} \quad (= \frac{\sigma_{xy}}{\lambda^+ - \sigma_y^2}). \quad (10)$$

It should also be noted that since the overlap ellipse is generally tilted, its area is not proportional to $\sigma_x \sigma_y$ as often assumed, but rather given by

$$S = \pi \sigma_x' \sigma_y' = \pi \sqrt{\sigma_x^2 \sigma_y^2 - \sigma_{xy}^2}. \quad (11)$$

Numerically the ratio, $\frac{\sigma_x' \sigma_y'}{\sigma_x \sigma_y}$, is very similar for the Cu + Cu and Au + Au systems at the same N_{part} , larger than 0.75, and increasing with increasing centrality so that for $N_{\text{part}} \geq 20$ it is larger than 0.9 in 200 GeV collisions.

< snip >

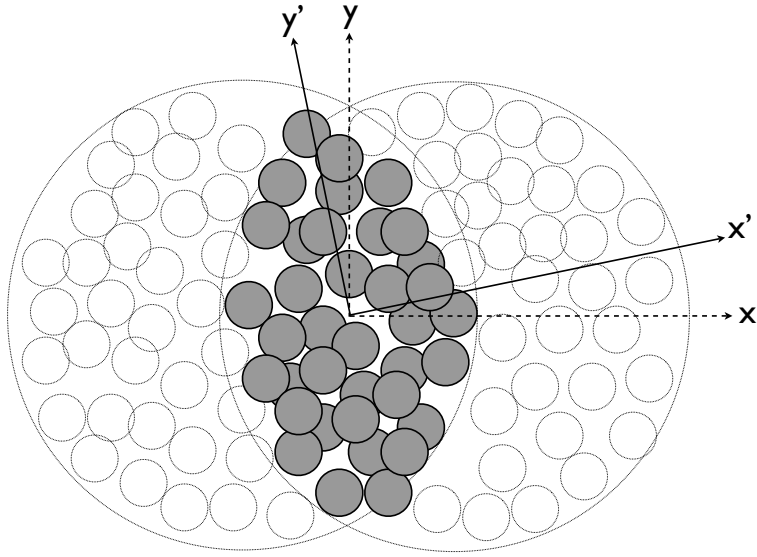


Figure 23: Schematic illustration of a nucleus–nucleus collision depicted in the transverse plane. The principal axes (x' and y') of the area formed by the participants are tilted with respect to the reaction plane given by the axes (x and y) of the transverse plane. Figure is taken from [11]

References

- [1] K. Homma, PHENIX analysis note 103
- [2] J. Nagle et al., PHENIX analysis note 113
- [3] J. Nagle et al., PHENIX analysis note 387
- [4] S. Milov, PHENIX analysis note 461
- [5] S. Milov, PHENIX analysis note 645
- [6] M. L. Miller, K. Reygers, S. J. Sanders and P. Steinberg, Ann. Rev. Nucl. Part. Sci. **57**, 205 (2007) [arXiv:nucl-ex/0701025].
- [7] J. Nagle et al., PHENIX analysis note 395
- [8] <https://www.phenix.bnl.gov/WWW/p/draft/reybers/glauber/>
- [9] K. Reygers et al., PHENIX analysis note 169 (official note calculating the N_{part} , N_{coll} , b, etc). and also Anlysis note 33 and 78.
- [10] B. Alver, M. Baker, C. Loizides and P. Steinberg, arXiv:0805.4411 [nucl-ex].
- [11] B. Alver *et al.*, Phys. Rev. C **77**, 014906 (2008)
- [12] R. S. Bhalerao, J. P. Blaizot, N. Borghini and J. Y. Ollitrault, Phys. Lett. B **627**, 49 (2005) [arXiv:nucl-th/0508009].
- [13] H. Heiselberg and A. M. Levy, Phys. Rev. C **59**, 2716 (1999)
- [14] H. Sorge, Phys. Rev. Lett. **82**, 2048 (1999)
- [15] Jean-Yves Ollitrault, Phys. Rev. D46, 229-245, 1992
- [16] S. Manly *et al.* [PHOBOS Collaboration], Nucl. Phys. A **774**, 523 (2006)
- [17] R. S. Bhalerao and J. Y. Ollitrault, Phys. Lett. B **641**, 260 (2006)
- [18] B. Alver *et al.* [PHOBOS Collaboration], Phys. Rev. Lett. **98**, 242302 (2007) [arXiv:nucl-ex/0610037].